Free Radical Research, January 2005; 39(1): 1–13

Taylor & Francis
Taylor & Francis Group

Differential responses of proliferative and non-proliferative leukemia cells to oxidative stress

EMMANUELLE PLANTIN-CARRENARD[1], MAGUY BERNARD[1], CHRISTIAN DERAPPE[2], ANNIE BRINGUIER[3], NATHALIE VADROT[3], GÉRARD FELDMANN[3], MARIE-JOSÉ FOGLIETTI[1], MICHÈLE AUBERY[2], & FRANÇOISE BRAUT-BOUCHER[2]

[1]*Laboratoire de Biochimie Générale et de Glycobiologie, U.F.R. des Sciences Pharmaceutiques et Biologiques, Université René Descartes Paris 5, 4 avenue de l'Observatoire 75006 Paris, France,* [2]*INSERM U-479, Faculté de Médecine Xavier Bichat, Université Denis Diderot Paris 7, 16 rue Henri Huchard, 75018 Paris France, and* [3]*INSERM U-481, Faculté de Médecine Xavier Bichat, Université Denis Diderot Paris 7, 16 rue Henri Huchard, 75018 Paris France*

Accepted by Dr Jean Cadet

This paper is dedicated to the memory of Dr. Catherine Pasquier

(Received 20th April 2004; revised 29th July 2004)

Abstract
The response of three human leukemia cell lines, the proliferative promonocyte THP-1 and the promyeloid HL60 cells and the non-proliferative phorbol ester-treated HL60 cells (HL60/PMA), to oxidative stress induced by *tert*-butylhydroperoxide (*t*-BHP) treatment was analyzed by fluorescence microplate assay, anti-oxidant enzyme activity measurements, high performance liquid chromatography, yopro-1/PI incorporation, poly (ADP-ribose) polymerase and caspase 3 cleavages. After *t*-BHP treatment, the non-proliferative HL60/PMA cells exhibited a weak increase in reactive oxygen species (ROS) production, a better preservation of thiol content, a decrease of glutathione peroxidase activity and a high ability to undergo necrosis rather than apoptosis. Submitted to the same treatment, the proliferative HL60 and THP-1 cells exhibited a high increase of ROS production, a moderate thiol depletion and a high percentage of apoptosis. Under thiol depleting conditions, the oxidative treatment of the HL60/PMA cells resulted in a high ROS production that reached levels similar to those of the two other cell lines and in cell death mainly by necrosis. In conclusion, these results that show proliferative phenotype is essential for cell response towards oxidative stress, are of particular interest in chemotherapy involving an oxidative mechanism.

Keywords: *Reactive oxygen species, anti-oxidant enzymes, thiols, apoptosis, leukemia cells*

Abbreviations: *CAT: Catalase, FMA: fluorescence microplate assay, GSH: glutathione, GPx: glutathione peroxidase, DCFH-DA: 2′,7′ dichlorofluorescin diacetate, HPLC: high performance liquid chromatography, mBrB: monobromobimane, NEM: N-ethyl maleimide, PARP: poly (ADP-ribose) polymerase, PMA: 12-O-*tetradecanoylphorbol 13-acetate, PI: propidium iodide, Cu/Zn SOD: cupper/zinc superoxide dismutase, Mn SOD: manganese superoxide dismutase, *t*-BHP: *tert*-butyl hydroperoxide, yopro-1: yopro-1 iodide

Introduction

Reactive oxygen species (ROS) are important cell mediators, continuously produced by cells, involved in cellular signaling mechanisms, cell proliferation and differentiation.[1] In normal cells, their production is equilibrated by anti-oxidant enzymes, thiols and glutathione cycle enzymes.[2,3] In pathological situations, the cellular intrinsic anti-oxidant defense can be overwhelmed by oxidative stress, resulting in high level of intracellular ROS and serious cellular damages.[4]

Correspondence: F. Braut-Boucher, INSERM U-479, Faculté de Médecine Xavier Bichat, Université Denis Diderot Paris 7, 16 rue Henri Huchard, 75018 Paris, France. Tel: 33-1-44-85-62-11. Fax: 33-1-44-85-62-07. E-mail: braut@bichat.inserm.fr

ISSN 1071-5762 print/ISSN 1029-2470 online © 2005 Taylor & Francis Ltd
DOI: 10.1080/10715760400013797

Three main anti-oxidant enzymes are present in cells: the Zn/Cu superoxide dismutase (SOD), the catalase (CAT) and the glutathione peroxidase (GPx). The SOD transforms superoxide anion $O_2^{\cdot -}$ into hydrogen peroxide (H_2O_2), which is then reduced in water and O_2, either directly by the CAT or by the GPx using the reduced glutathione (GSH) as co-substrate; the GPx is also capable of reacting with lipid hydroperoxides. Glutathione cycle enzymes are a complex cellular system able to maintain an adequate GSH and thiol levels in cells. Yet, the GSH level depends on the availability of the cysteine, a precursor of GSH and thus, the redox system involving glutathione plays a critical role in the scavenging of the ROS, in the maintaining of cellular homeostasis and consequently in cell viability.

Oxidative stress may result in cell death by apoptosis or necrosis.[5–8] Apoptosis or programmed cell death is a highly regulated process including several proteases, such as caspases and characterized by proteolysis, chromatin condensation, nuclear and DNA fragmentation. In contrast, necrosis is an un-programmed cell death occurring after cell exposition to a toxic molecule and characterized by total cell destruction including the plasma membrane, the nucleus and the other cell organelles.

Under exogenous oxidative stress conditions, cells are able to modify their metabolic pattern to increase their anti-oxidant defenses in order to restore the balance between anti-oxidant enzyme expression, GSH biosynthesis and ROS production. These modifications could be considered as adaptive response of cells towards oxidative stress and they could be different according to the cell status. Especially, it was shown that cell differentiation is accompanied by changes in the redox state of cells.[9] Although a lot of work has been published to describe the relationship between oxidative stress and apoptosis triggering, only few of them deal with the relation between apoptosis and cell differentiation or cell proliferation.

To analyse such possible relation, we used as *in vitro* cellular model, three human leukemia cells lines including different steps of cell differentiation: the proliferative promonocytic THP-1 cells,[10] the proliferative promyeloid HL60 cells,[11] and the non-proliferative HL60/PMA cells obtained by differentiation into monocytic phenotype by phorbol ester treatment (PMA).[12] This model was recently used by Moon et al.[13] The response to oxidative stress, induced by a chemical agent, the *tert*-butylhydroperoxide (*t*-BHP), was characterized by changes in intracellular ROS production, thiol content and apoptosis induction, all measured by methods that we recently described.[7,14,15] Moreover, activity and expression of three anti-oxidant enzymes were determined by biochemical methods and western blot analyses. Results showed important differences in cell response towards oxidative stress between proliferative and non-proliferative cells, especially as regards apoptosis and necrosis.

Materials and methods

Materials

Cell culture media and supplements were purchased from Invitrogen—Life Technologies (Grand Rapids, NY, USA). Phorbol 12-myristate 13-acetate (PMA), nitro blue tetrazolium (NBT), *t*-BHP at 70% (v/v) in aqueous solution, trypan blue solution, the protease inhibitor cocktail, the reagents used for the determination of enzyme activities and thiol measurement by HPLC were purchased from Sigma (Saint Louis, MO, USA). Fluorescent probes, 2′,7′ dichlorofluorescin diacetate (DCFH-DA), monobromobimane (mBrB), yopro-1 and propidium iodide (PI) were purchased from Molecular Probes (Eugene, OR, USA). The mouse IgG2a anti-β actin monoclonal antibody, used as internal control in western blots, was obtained from Sigma. The mouse IgG1 anti-human glutathion peroxidase monoclonal antibody (clone 347) and the rabbit IgG anti-human CAT polyclonal antibody were purchased from Calbiochem (VWR International SAS, Fontenay-sous-Bois, France). The rabbit IgG anti-human Cu/Zn SOD polyclonal antibody, the rabbit IgG anti-human Mn SOD polyclonal antibody, the donkey anti-rabbit IgG-HRP and the goat anti-mouse IgG-HRP were purchased from Stressgen (Victoria BC, Canada). The goat anti-rabbit IgG-HRP was obtained from Immunotech (Marseille, France). The goat anti-U1 small ribonucleoprotein (U1 SnRP 70) was obtained from Santa Cruz Biotechnology (Santa Cruz, CA, USA) and the anti-caspase 3/CPP32 from AbCys (Paris, France). The mouse IgG1 anti-PARP antibody (clone C2-10) was purchased from Pharmingen International (San Diego, CA, USA). The western blot detection system was from Amersham (Amersham International, Buckinghamshire, UK). Rnase A and DAPI were from Sigma. Polystyrene flasks and 96-well culture plates were obtained from Falcon (Becton Dickinson, Le Pont de Claix, France).

Cell culture and cell differentiation

THP-1 cells (ECACC reference n° 88081201)[10] and HL60 cells (ECACC reference n° 85011431)[11] were cultured in RPMI 1640 medium supplemented with 10% heat-inactivated foetal calf serum (FCS), antibiotics (100 μg/ml streptomycin, 100 U/ml penicillin) and 2 mM L-glutamine, in a humidified atmosphere containing 5% CO_2 at 37°C. The cells were cultured either into 75 cm^2 tissue culture flasks at the initial concentration of 3×10^5 cells/ml or in 96-well flat bottom microplates at 5×10^4 cells/well.

Cell viability was assessed using trypan blue exclusion test. HL60 cells were used between the fifteenth and fortieth passage.

The HL60 differentiation into non-proliferative monocytic phenotype was obtained by treatment with phorbol ester (PMA) for three days at a final concentration of 50 ng/ml added to HL60 suspension.[12] The NBT reduction assay was used to verify cellular differentiation status.[16] Moreover, differentiated cells became adherent and exhibited intracellular blue-black formazan deposits.

For cell characterization, cytospin slide preparation of 0.15 ml suspension at 10^6 cells/ml was obtained using a Shandon Cytospin 3 then stained with May-Grunwald-Giemsa reagent before microscopic examination.

Oxidative stress induction

Oxidative stress was induced by *t*-BHP treatment performed on cells cultured in 96-well microplates, as previously described.[15]

ROS production was measured *in situ* by labeling the cells with the fluorogenic DCFH-DA probe at 5 μM for 30 min (37°C). The fluorescence signal was quantified in a fluorescence plate reader (Fluostar II BMG, Champigny/Marne, France) at λ_{exc} 485 nm and λ_{em} 538 nm. Data were collected directly in arbitrary fluorescence units (AFU) and results were expressed as increased percentages to untreated cells (100%).

Determination of enzyme activity and expression

Enzyme activity assays, protein determination and western blot analyses were carried out on untreated and *t*-BHP-treated cells (5, 30 and 60 min). After treatments, adherent HL60/PMA cells were softly detached from culture flasks using a rubber policeman and centrifuged and non-adherent THP-1 and HL60 cells were directly centrifuged. Cell pellets were washed with PBS and cell concentration adjusted at 2×10^6 cell/ml in PBS. For protein determination and enzyme activity assays, cellular extracts were obtained by sonication in pulsed mode 50 W at 4°C, for 1 min performed in PBS. Then, samples were centrifuged at 4°C for 15 min at 15,000*g* and supernatants kept at − 80°C until use.

The protein concentration was determined by the bicinchoninic acid assay (BCA) from Pierce (Rockford, IL, USA).

The SOD (EC 1.15.1.1) activity was assayed by the method of Mc Cord and Fridovitch[17] and the CAT (EC 1.11.1.6) activity by the method of Johansson and Borg.[18] The GPx (EC 1.11.1.19) activity was determined using the Ransel® GPx Kit (Randox, UK), according to the manufacturer's recommendations. Enzyme activities were expressed in U/mg of protein: one unit of the enzyme was defined as mmol of substrate degraded per min per mg of protein.

Anti-oxidant enzyme expression was analyzed by western blots, as previously described.[19] Cell pellets obtained as indicated above were lysed in presence of detergent. Cellular proteins were separated by sodium dodecyl sulfate polyacrylamide gel electrophoresis (SDS PAGE) and electrophoretically transferred to a nitrocellulose membrane. To block free sites, the membrane was incubated in 5% non-fat dry milk in PBS containing 0.1% Tween 20. The blots were then probed with the appropriate antibodies. A second HRP-conjugated antibody was used for a chemiluminescent detection (ECL, Amersham), according to the manufacturer's instructions. Then, membranes were exposed to Kodak X-OMAT UV film and band intensity was semi-quantified with Scion® software. Protein loading reproducibility was assessed by analysis of β-actin.

Thiol determination

Fluorescence microplate assay (FMA). Intracellular thiol levels were measured by the fluorescent probe mBrB, which forms a fluorescent adduct with thiol groups.[20] Cells were labeled by incubation at 37°C for 10 min in the dark with 30 μM mBrB. Fluorescence signal variation was assessed by microplate titrating reader at λ_{exc} 390 nm and λ_{em} 460 nm. Results, obtained directly in AFU, were expressed as percentages to untreated cells (100%).

HPLC analysis. Glutathione and cysteine levels were measured by high performance liquid chromatography (HPLC) according to the method of Jacob et al.[21] Cells were washed with PBS, centrifuged and pellets lysed with 1 ml of cold distilled water. After centrifugation at 15,000*g* for 15 min at 4°C, the supernatant was rapidly submitted to derivatization to minimize GSH degradation. Thiol containing extracts were treated by tri-n-butylphosphine solution 10% in N,N-dimethylformamide and proteins precipitated by trichloracetic acid solution at 10% containing 1 mM EDTA. Then, thiols were labeled with 4.6 mM 7-fluoro-2,1,3-benzodiazole-4-sulfonamide in 0.125 mM borate buffer containing 4 mM EDTA and analyzed on a greffed silice C18 microbondapak column (Waters, St-Quentin-en-Yvelines, France) by isocratic elution with a mobile phase of 0.1 mM phosphate buffer (pH 3.2) containing 10% acetonitrile. Fluorescence intensity was monitored at λ_{exc} 385 nm and λ_{em} 515 nm. Integration of chromatograms was accomplished using Millenium® software (Waters).

Standard curves were obtained from three standard solutions containing GSH (150, 75 and 50 μM) and L-cysteine (50, 25 and 5 μM). The solutions were prepared by dilution of 1 mM stock solutions in acid

phosphate buffer. The reduction control solution contained 100 μM oxidized glutathione and 50 μM L-cystin. The internal standard was 2.5 mM N-acetyl-cysteine in 0.9% NaCl containing 0.4 mM EDTA. Detection limit was determined at 0.5 μM GSH or cysteine.

Thiol depletion

Thiol depletion was obtained by treatment of cells with the alkylating reagent N-ethylmaleimide (NEM), used at 0.1 or 0.2 mM for 15 min and controled by HPLC, as indicated above. After NEM-depleting treatment, cells could be submitted or not to the *t*-BHP treatment.

Protective treatment assay

Protection against ROS was assessed by pre-treatment of cells by two thiol compounds, glutathione and cysteine.[22] The thiol solutions were prepared just before experiment by dilution in PBS at defined concentration and after adjustment of the pH at 7.4. Protective effects were evaluated by the decrease of ROS production measured by FMA.

Apoptosis

Apoptosis was induced by treatment of cells (1×10^6 cells/ml HBBS) with 1 mM *t*-BHP for 1 h at 37°C, followed by 2 h incubation in HBSS without *t*-BHP, as already described.[15] To assess the consequences of thiol depletion on apoptosis induction, cells were incubated with 0.1 mM NEM for 15 min followed by 2 h incubation in HBSS at 37°C. Then, cells were washed and re-suspended in HBSS and cell morphology was controlled by microscopic examination. Apoptosis was assessed by FMA and immunodetection of PARP and caspase 3 cleavages.

Fluorescence microplate assay. Cells cultured in 96-well plate were labeled with fluorescent probes yopro-1 (5 μM) and PI (10 μg/ml) as previously described.[15] In these conditions, viable cells excluded both yopro-1 and PI probes, apoptotic cells took up only yopro-1 probe and necrotic cells were labeled by both yopro-1 and PI probes. The following optimum wavelengths for yopro-1 were λ_{exc} 485 nm and λ_{em} 538 nm and for PI, λ_{exc} 590 nm and λ_{em} 630 nm. Results were expressed as percentages of increase of fluorescent signal in treated cells compared to untreated cells.

PARP and caspase 3 cleavages. PARP and caspase 3 cleavages were performed according to the method described by Lamboley et al.[21] Briefly, at the end of the incubation corresponding to each treatment, cells were removed from the flasks and centrifuged at 500*g* for 5 min. Pellets were re-suspended in 1 ml of PBS and centrifuged again. Supernatants were carefully discarded and pellets were weighted and frozen at 80°C until use. Cytoplasmic and nuclear extracts were separated as previously described.[22] Cytoplasmic or nuclear samples corresponding to 2 mg of cell pellets were submitted to SDS PAGE for immunodetection, as indicated in the last paragraph of determination of enzyme activity and expression section. Reproducibility was assessed by analysis of β-actin for cytoplasmic proteins and U1 SnRNP 70 for nuclear proteins.

Statistical analysis

Mean values were calculated from data of three separate experiments done in triplicate and reported as mean ± SEM. The statistical significance of the differences between observed values was determined by Student's *t*-test. Values of p inferior to 0.05 were considered statistically significant.

Results

ROS production

For the three cell lines cell viability was routinely assessed by trypan blue exclusion in all experiments and cells exhibiting viability lower than 90% were discarded. ROS production was measured by FMA using DCFH-DA probe. For both proliferative THP-1 and HL60 cell lines and non-proliferative HL60/PMA cells, *t*-BHP treatment resulted in time- and dose-dependent increase of the ROS production (data not shown). Table I reported optimum results obtained for ROS production using 1 mM *t*-BHP for 1 h.

Thus, proliferative THP-1 and HL60 cells exhibited an important increase of ROS production after the oxidative treatment (177 and 192%, respectively) in comparison to the non-proliferative HL60/PMA cells (Table II) which exhibited a moderate ROS production (38%).

Table I. FMA measurements of ROS production.

	THP-1 cells	HL60 cells	HL60/PMA cells
Untreated cells	459 ± 41	1685 ± 135	1293 ± 103
t-BHP treated cells	1271 ± 102	4920 ± 394	1784 ± 143

Cells were incubated for 1 h with 1 mM *t*-BHP. ROS production was measured using the fluorogenic DCFH-DA probe (5 μM). Fluorescence emission was measured on a fluorescence plate reader at λ_{exc} 485 nm, λ_{em} 538 nm and expressed in arbitrary fluorescent units (AFU). Values are means ± SE from three different experiments done in triplicate.

Table II. Protection against ROS production after GSH or Cys external cell pre-treatment.

		THP-1 cells (%)	HL60 cells (%)	HL60/PMA cells (%)
GSH (mM)	0	100 ± 4.8	100 ± 5.0	100 ± 6.1
	31	107 ± 5.0	66 ± 3.3	49 ± 3.0
	62	97 ± 5.2	62 ± 3.1	47 ± 2.5
	125	93 ± 5.0	49 ± 2.0	39 ± 1.9
	250	75 ± 4.1	30 ± 1.8	26 ± 1.3
Cys (mM)	0	100 ± 5.1	100 ± 5.1	100 ± 5.0
	31	103 ± 5.4	96 ± 4.9	49 ± 6.6
	62	109 ± 5.2	72 ± 4.3	21 ± 1.1
	125	89 ± 4.8	63 ± 4.7	32 ± 2.2
	250	44 ± 4.3	46 ± 3.8	27 ± 1.9

Cells were incubated for 1 h with indicated GSH and Cys concentrations and submitted to *t*-BHP treatment (1 mM for 1 h). ROS were measured by FMA using DCFH-DA probe. Results were expressed in percentages of ROS production in protected cells in comparison to unprotected cells noted as 100%. Values are means ± SE from three different experiments done in triplicate.

Involvement of endogenous defense systems

Modulation of enzyme activities. The effects of the *t*-BHP treatment on SOD, CAT and GPx activity were measured in the three cell lines (Figure 1). The SOD activity reached 1 U/mg protein in non-proliferative HL60/PMA cells versus 3.5 and 2.7 U/mg protein in proliferative THP-1 and HL60 cells, respectively. After *t*-BHP treatment, the SOD activity decreased in THP-1 and HL60 cells, whatever the incubation period (Figure 1A). For example, after 60 min of 1 mM *t*-BHP treatment, SOD activity decreased by 63 and 56% in HL60 and THP-1 cells, respectively. On the contrary, in HL60/PMA cells, no significant change was measured.

The basal CAT activity was higher in THP-1 cells (67 U/mg protein) than in HL60 and HL60/PMA cells (35 and 12 U/mg protein, $p < 0.05$, respectively) and after 1 h of 1 mM *t*-BHP treatment (Figure 1B) a strong increase of the CAT activity was observed in HL60 cells (146%, $p < 0.05$ versus untreated cells) to reach similar activity as this of THP-1 cells.

In untreated cells, the GPx activity was higher in HL60/PMA cells (0.39 U/mg protein) than in THP-1 and HL60 cells (0.18 and 0.07 U/mg protein, $p < 0.05$ respectively). The *t*-BHP treatment induced at 30 min a 76% decrease of GPx activity in HL60/PMA cells (Figure 1C). For the two other cell lines, changes in GPx activity were very low.

Although of the probability of *de novo* protein synthesis for the anti-oxidant enzymes was low over 1 h incubation time, such possibility cannot be *a priori* rejected. Consequently, the western blots showing Cu/ZnSOD, MnSOD, CAT and GPx protein expression at *t*-BHP treatment times 0, 5, 30 and 60 min have been performed. Results in Figure 1 show that no significant changes in both SOD and CAT expression occurred during the *t*-BHP treatment. On the contrary, for GPx expression, some differences were observed between the three cell lines: no GPx expression change in THP-1 cells, no GPx expression in HL60 cells and a decreasing expression in HL60/PMA cells after 30 min of *t*-BHP treatment. The absence of GPx detection in HL60 cells may be in relation to the low GPx activity measured for these cells. The decreasing GPx expression noticed for HL60/PMA cells may result in the decreasing GPx activity observed for these cells, probably due to protein degradation under the oxidative stress conditions.

Thus, *t*-BHP treatment induced several modifications in anti-oxidant enzyme activities, particularly an important increase of CAT activity for the HL60 cells and a decrease of GPx activity in the HL60/PMA cells.

Modulation of intracellular thiol levels. The total thiol compounds were assessed by FMA using the fluorescent probe mBrB. The cells were treated for 1 h with 1 mM of *t*-BHP and a moderate decrease of mBrB signal was observed for the THP-1 cells (25%) and the HL60 cells (20%), in comparison to untreated cells (Figure 2A). For the HL60/PMA cells, thiol depletion was not significant.

HPLC analysis was used to measure specifically GSH and cysteine concentrations. Results showed that the basal levels of intracellular GSH and cysteine were weak in the non-proliferative HL60/PMA cells (1.5 and 3.7 μmol/mg proteins, respectively, data not shown) in comparison to the proliferative THP-1 cells (15.1 and 17.1 μmol/mg proteins, respectively) and HL60 cells (34.1 and 12.9 μmol/mg proteins, respectively). For the HL60/PMA cells, the GSH and cysteine levels (between 0.5 and 1.0 μmol/mg proteins) remained low after *t*-BHP treatment and consequently not take in count.

After applying the *t*-BHP treatment (1 mM for 1 h), GSH level decrease was observed in THP-1 cells (60%) and only 10% in HL 60 cells (Figure 2B). Regarding the cysteine pool, its decrease was moderate and reached 36% in the THP-1 cells and 39% in the HL60 cells (Figure 2B).

Effects of thiol depletion on ROS production. To estimate the role of thiols in cell defense against oxidative stress and associated effects, a thiol depletion was obtained using NEM treatment at concentrations of 0.1 or 0.2 mM. After depletion, cells were submitted or not to *t*-BHP treatment and results are reported in Figure 3.

In the three cell lines, NEM treatment induced an important thiol depletion, which was accentuated by *t*-BHP treatment for the HL60/PMA and the THP-1

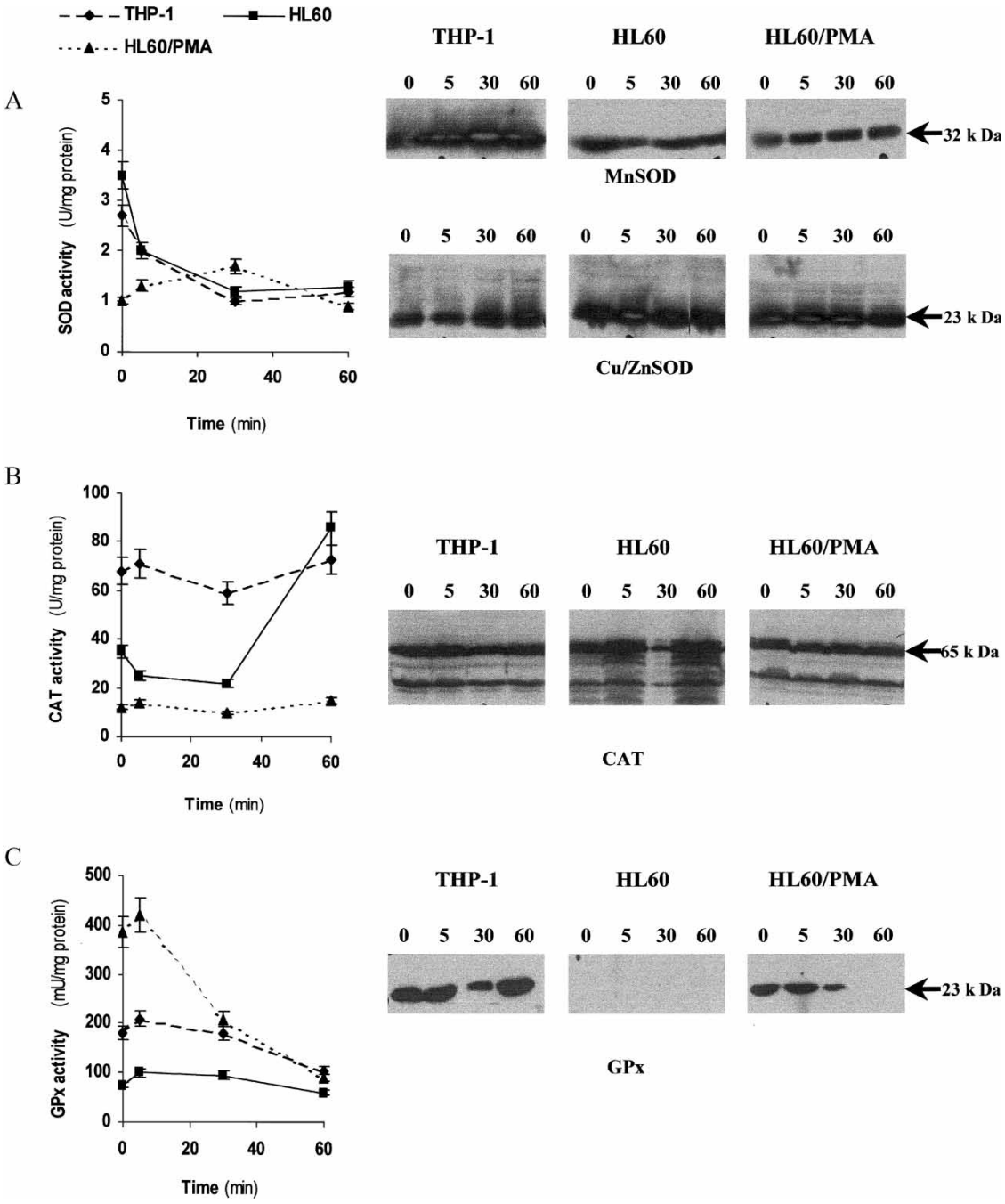

Figure 1. Time-course of the effect of *t*-BHP treatment on anti-oxidant enzyme activity and expression in each cell line. Experiments were carried out on cell lysates after 0, 5, 30 and 60 min of *t*-BHP treatment. SOD activity was assessed using reduction of cytochrome c by superoxide radicals generated by the hypoxanthine/xanthine oxidase system.[17] CAT activity was determined by the method of Johanson and Borg.[18] GPx activity was determined using the Ransel® GPx kit. Each data point represents the mean ± SE of three separate experiments. Enzyme expression was analyzed by western blots, as described in "Material and Methods" section. Mn SOD give a band at 32 kDa, Cu/Zn SOD at 23 kDa, CAT at 65 kDa and GPx at 23 kDa. β-actin was used as control (bands not shown). **A**: SOD activity and Mn SOD and Cu/Zn SOD expression; **B**: CAT activity and expression; **C**: GPx activity and expression.

cells. For HL60 cells, thiol depletion did not change after the oxidative treatment.

The ROS production obtained after NEM treatment was increased in a dose-dependent manner in the three cell lines. In both proliferative THP-1 and HL60 cell lines, the ROS production obtained by t-BHP treatment was not modified significantly after thiol-depletion (Figure 3). In contrast, in the non-proliferative HL60/PMA cells, *t*-BHP treatment performed on depleted cells resulted in a dramatic increase of ROS production, in comparison to undepleted cells, reaching levels similar to those of the two proliferative THP-1 and HL60 cell lines.

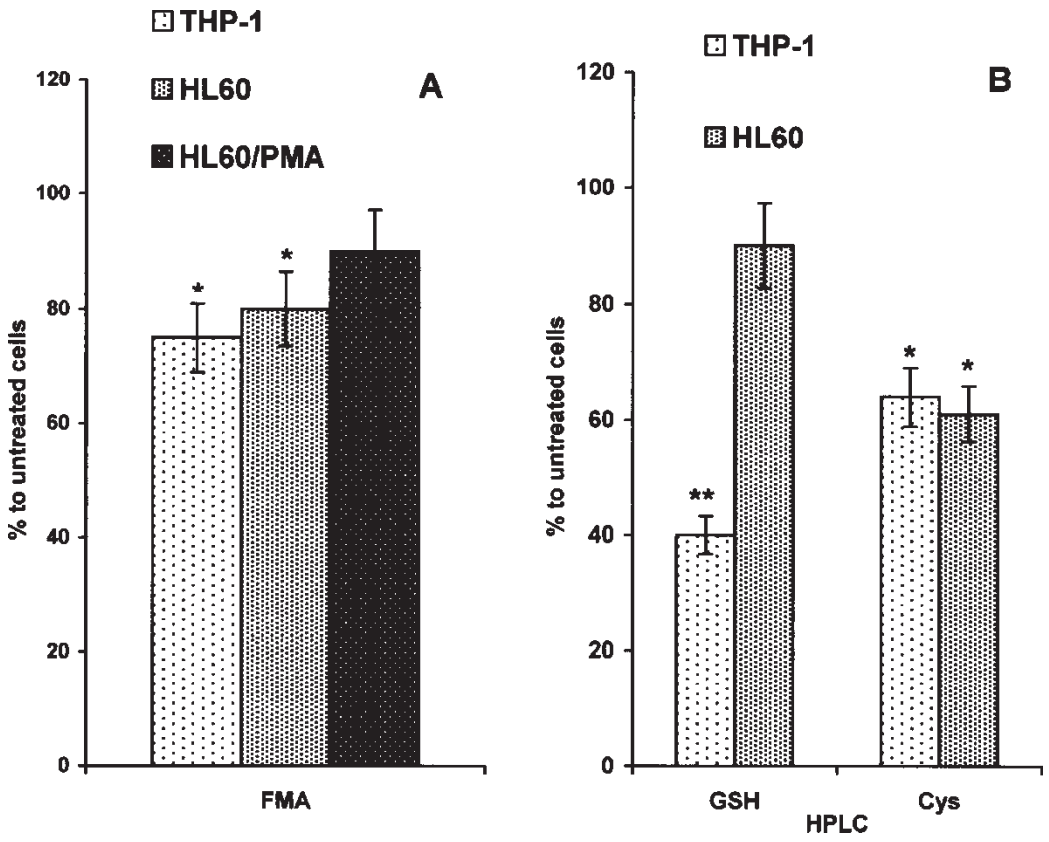

Figure 2. Total thiols, GSH and cysteine in cells after oxidative treatment. Thiol compounds were measured before and after treatment with 1 mM *t*-BHP for 1 h. **A**: FMA measurements of thiols using the mBrB fluorescent probe. **B**: HPLC measurements of GSH and cysteine, as described in "Material and Methods" section. Results are expressed as percentages of thiol compounds in treated cells compared to untreated cells and represent the mean ± SE of three separate experiments. $^{\star}p < 0.05$, $^{\star\star}p < 0.01$.

Induction of apoptosis or necrosis

Effect of t-BHP treatment. To assess cell death by apoptosis or necrosis, cells were treated by 1 mM *t*-BHP for 1 h and then incubated for 2 h, in absence of *t*-BHP. Apoptosis and necrosis were determined by double labeling of cells with two fluorescent probes: yopro-1 to measure apoptosis and PI to measure necrosis (Figure 4A). Results were expressed as increasing percentages of fluorescent signal in comparison to untreated cells. After *t*-BHP treatment, the increase of the fluorescent yopro-1 signal (apoptosis) was significantly higher in both proliferative cell lines (95 and 110% for THP-1 and HL60 cells, respectively), than in the non-proliferative HL60/PMA cells (30%). In contrast, the increase of the PI signal (necrosis) was about 3 fold higher in non-proliferative HL60/PMA cells, compared to the two proliferative HL60 and THP-1 cell lines, revealing that necrosis was predominant over apoptosis in the non-proliferative cells, after *t*-BHP treatment.

Apoptosis triggered by oxidative treatment was further analyzed by cleavage of PARP in nucleus (Figure 4B) and caspase 3 in cytosol (Figure 4C). PARP expression was very different according to the three cell lines. As shown in Figure 4B, in untreated cells, a strong PARP expression was observed in THP-1 cells, in comparison to the two other cell lines. In the three untreated cell lines, there is a low spontaneous cleavage of PARP characterized by the apparition of an 85 kD band. The *t*-BHP-treatment resulted in PARP cleavage in proliferative HL 60 cells, the intensity of the 85 kD band, semi-quantified by densitometry, was increased by 120%, in comparison to untreated cells. For the THP-1 cells, no significant changes were observed in PARP cleavage be fore and after *t*-BHP treatment. For the HL60/PMA cells, the intensity of the 85 kD cleaved band was very low; this could be related to the high necrosis level observed for these cells.

Expression of caspase 3 was analyzed by immunoblot and apoptosis was characterized by the cleavage of the 32 kD caspase 3 band to the 18 kD band. As shown in Figure 4C, it has been observed that the level of caspase 3 expression was higher in the non-proliferative HL60/PMA cells than in the two other proliferative cell lines. In comparison to untreated cells, *t*-BHP treatment resulted in a 3 fold increase of the intensity of the 18 kD band in both proliferative cell lines, while in non-proliferative HL60/PMA cells only a 1.5 fold increase was observed.

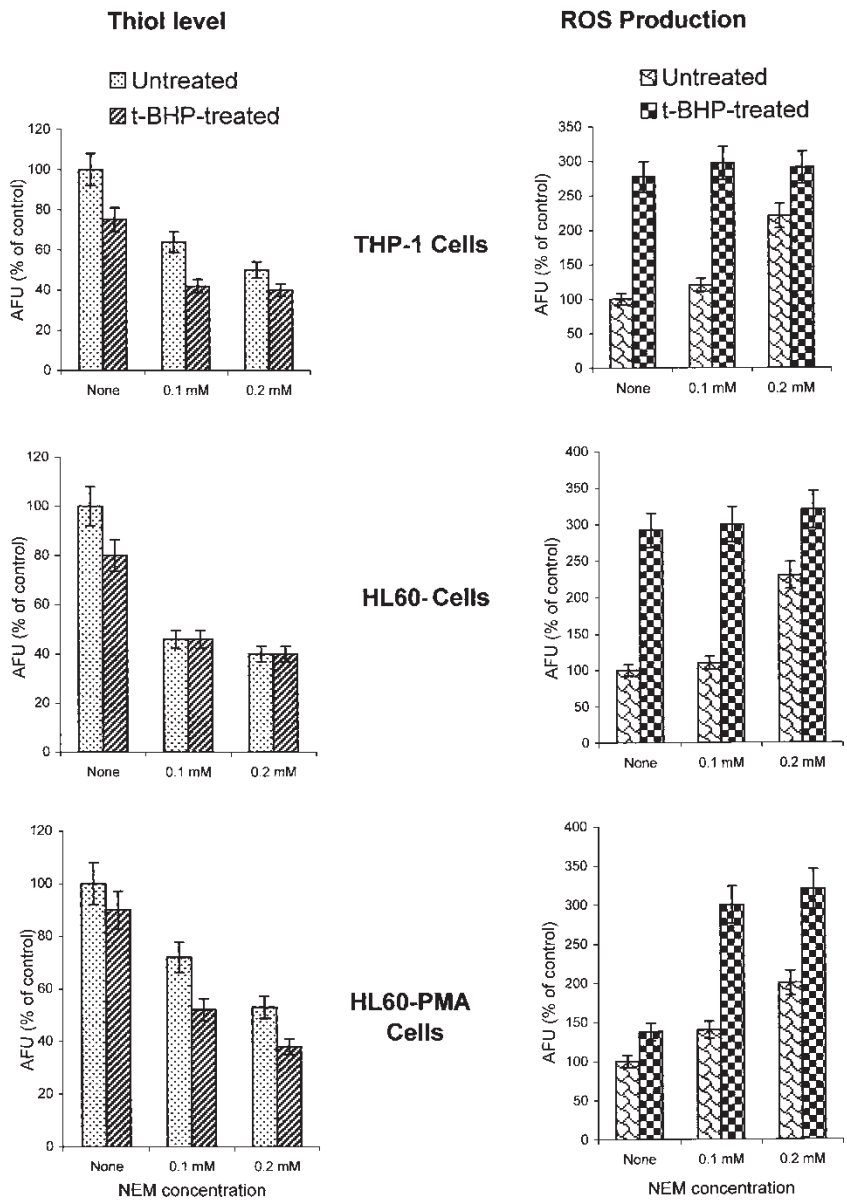

Figure 3. ROS production and thiol level in thiol-depleted THP-1, HL60 and HL60/PMA cells, before and after *t*-BHP treatment. Cells were pre-treated by 0.1 or 0.2 mM NEM for 15 min, then treated or not by 1 mM *t*-BHP for 1 h. ROS production and thiol level were determined by FMA using the DCFH-DA and mBrB fluorescent probes, respectively, as indicated in "Materials and Methods" section. Results are expressed as percentages of AFU in treated cells compared to control cells (control cells were not treated either with NEM or *t*-BHP) and represent the mean ± SE of three separate experiments.

Thus, results obtained from FMA and PARP and caspase 3 cleavages indicated that the oxidative treatment induced more apoptosis in proliferative cell lines than in the non-proliferative one.

Effect of thiol depletion on cell death. As shown by Macho et al.[24] thiol depletion was able to induce cell death. To examine this possibility, cells were treated with 0.1 mM NEM for 15 min and incubated for 2 h in HBSS. Analyses were run using the yopro-1/PI incorporation (Figure 5A), PARP (Figure 5B) and caspase 3 (Figure 5C) cleavages.

A marked increase of yopro-1 signal was observed in the two proliferative THP-1 and HL60 cell lines, while no significant increase of yopro-1 signal was noted for the non-proliferative HL60/PMA cells (Figure 5A). Conversely, only the HL60/PMA cells exhibited a marked increase of PI signal, indicating that these cells underwent necrosis rather than apoptosis.

A strong expression of PARP in THP-1 cells and caspase 3 in HL60/PMA cells was observed before NEM treatment. After NEM treatment an important cleavage of PARP in HL60 cells, a weak PARP cleavage in HL60/PMA cells and a weak caspase 3 cleavage in THP-1 and HL60/PMA cells were observed (Figure 5B and C).

Results showed that thiol depletion induced apoptotic effects in both proliferative HL60 and

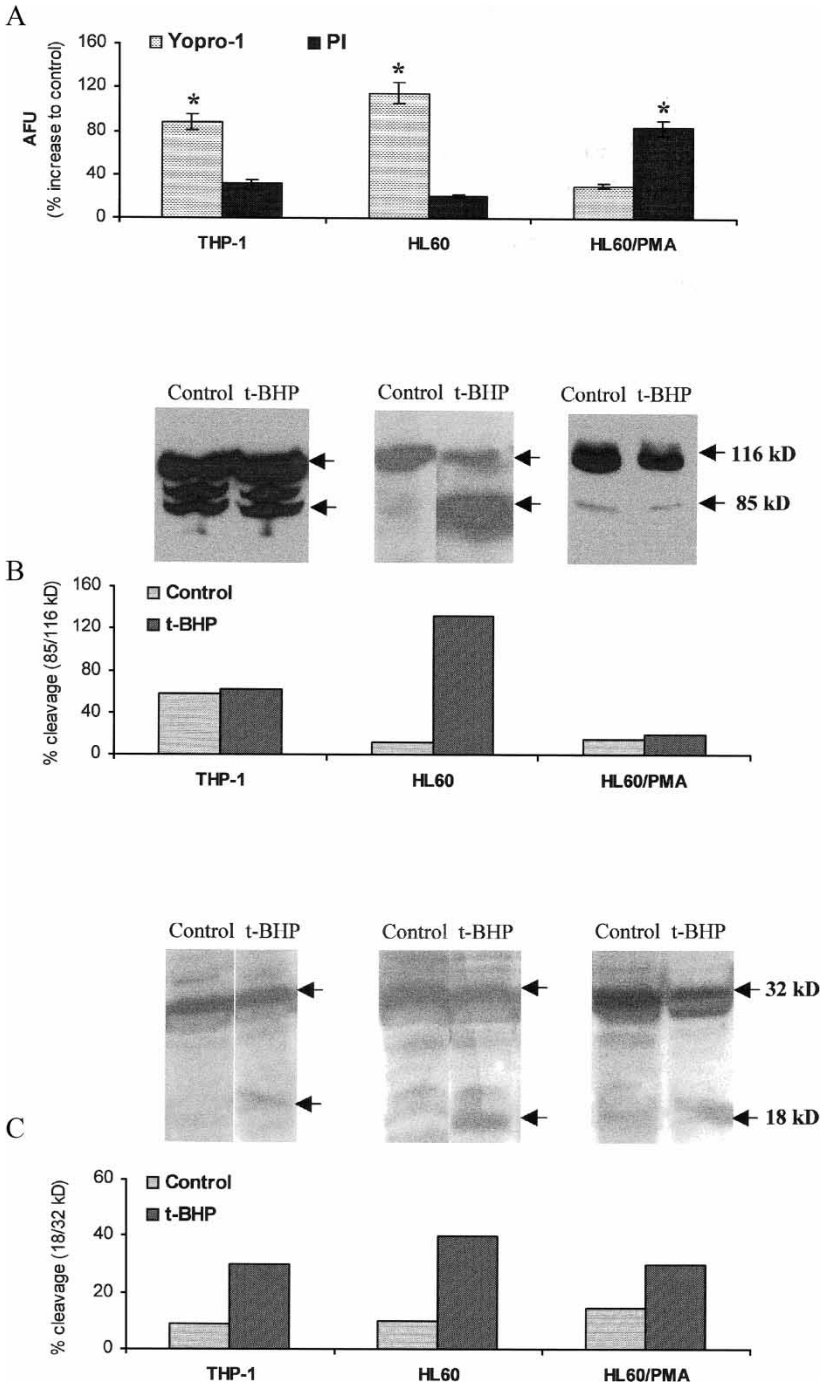

Figure 4. Apoptosis triggering by *t*-BHP treatment. Cells were incubated with 1 mM *t*-BHP for 1 h followed by a 2 h incubation in absence of *t*-BHP. **A**: Fluorescence measurement. Cells were stained with 5 μM yopro-1 and 10 μg/ml of PI at 4°C for 30 min. The fluorescence emission was measured on a fluorescence plate reader at λ_{exc} 485 nm, λ_{em} 538 nm for yopro-1 and λ_{exc} 590 nm, λ_{em} 630 nm for PI. Results were expressed as percentages of increase of arbitrary fluorescent units (AFU) in comparison to control. Figure 4 A represents the mean ± SE of three separate experiments. $^{\star}p < 0.05$. **B**: PARP cleavage. Nuclear extracts were separated on 6% SDS-PAGE (50 μg of protein per lane) followed by transfer on nitrocellulose membrane. Immunodetection of PARP cleavage was done using the mouse IgG1 anti-PARP antibody, followed by chemiluminescence detection using the HRP-conjugated goat anti-rabbit antibody and the ECL western blot detection system from Amersham. After staining by chemiluminescence, 116 and 85 kD band intensities were quantified by densitometry using Scion® software. Results were expressed as percentages of cleavage 85/116 kD) and given as histograms below the blots. **C**: Caspase 3 cleavage. Cytosolic extracts were separated on 15% SDS-PAGE (50 μg of protein per lane) and transferred on nitrocellulose. Immunodetection of caspase 3 cleavage was done using the rabbit anti-active caspase 3 antibody and the same chemiluminescence system as for the PARP cleavage. After staining, 18 and 32 kD band intensities were quantified by densitometry as described for PARP. Results were expressed as percentages of cleavage (18/32 kD) and given as histograms below the blots.

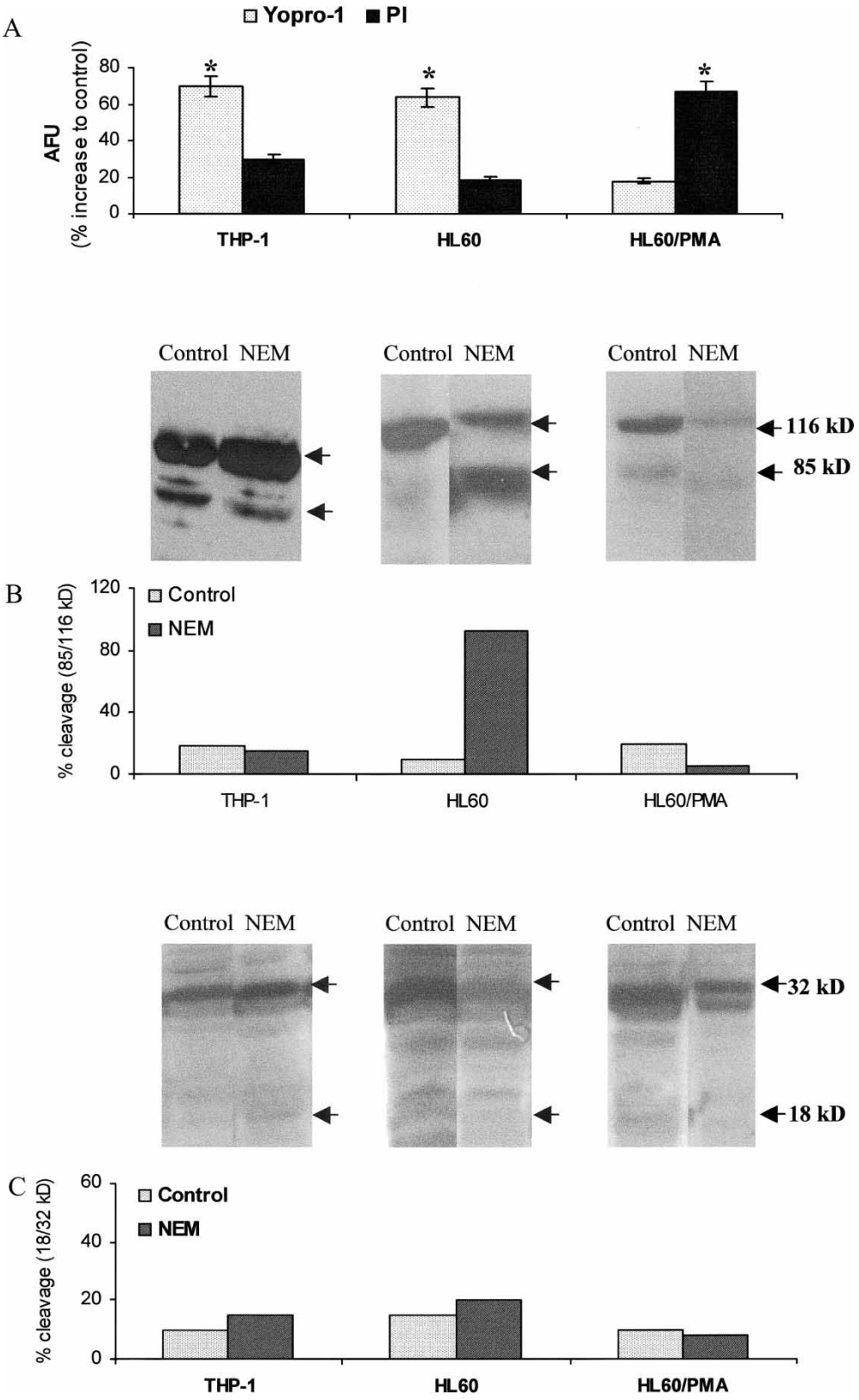

Figure 5. Apoptosis triggering by NEM treatment. Apoptosis was induced by treatment of cells with 0.1 mM NEM for 15 min, followed by a 2 h incubation in HBSS. Figure 5A represents the mean ± SE of three separate experiments. $*p < 0.05$. **A**: Fluorescence measurement was performed as indicated in Fig. 4A legend. **B**: PARP cleavage was performed as indicated in Fig. 4B legend. **C**: Caspase 3 cleavage was performed as indicated in Fig. 4C legend.

THP-1 cells and predominantly cell death by necrosis in the non-proliferative HL60/PMA cells.

Protective effects of glutathione and cysteine

In order to prevent the effects of oxidative treatment, cells were pre-treated for 1 h with different concentrations of GSH or cysteine. After pre-treatment, the cells were submitted to 1 mM *t*-BHP treatment for 1 h and the ROS production was measured by FMA. Results of ROS production in Table II, expressed in percentages of AFU in protected cells in comparison to unprotected cells, showed distinct effects, according to the cell type and the protecting agent. Any significant protective effect of GSH can be observed before 250 mM GSH for the THP-1 cells (25%). In contrast, a marked protective effect was measured from 31 mM GSH for HL60 and HL60/PMA cells (34 and 51%, respectively). At 250 mM GSH, the protective effect reached 70 and 74% for HL60 and HL60/PMA cells, respectively. The protective effect of cysteine was observed on HL60/PMA cells from 31 mM (51%) and reached 79% with 62 mM cysteine. For the two other cell lines, 250 mM cysteine was required to obtain a genuine protective effect (56 and 54% for THP-1 and HL60 cells, respectively).

Discussion

In this study, we have compared the responses to an exogenous oxidative treatment of three human leukemia cell lines at different steps of differentiation, two proliferative ones (THP-1 and HL60 cells) and one non-proliferative (HL60/PMA cells). The more differentiated HL60/PMA cell line became adherent after PMA treatment, but keep several characteristics of undifferentiated cells.[25] In this paper, we observed different adaptive responses towards the oxidative stress, according to the cell status.

As regards ROS production, important differences were observed between the two proliferative HL60 and THP-1 cells and the non-proliferative HL60/PMA cells, suggesting varying levels of anti-oxidant capacities according to the proliferation state. In parallel, *t*-BHP treatment resulted in moderate decrease in thiol level in the three cell lines, 20% in the two proliferative cell lines and 10% in the non-proliferative one, as shown by FMA using mBrB as fluorescent probe. Besides, HPLC measurements exhibited different individual variations between two main thiols, GSH and Cys. Particularly, HL60 cells have a high basal level in GSH, which exhibited a moderate decrease (10%) after *t*-BHP treatment; this protection against oxidative stress could be due to the presence of other specific anti-oxidant defenses, such as thioredoxine or metallothioneins, as previously proposed.[26,27] On the contrary, GSH level in THP-1 cells, which was lower than in HL60 cells, strongly decreased (60%) after *t*-BHP treatment and thus was not sufficient to protect cells from the oxidative stress. Concerning the HL60/PMA cells, their basal levels in GSH and cysteine were too low to take into account possible variations after the oxidative treatment.

Another adaptive response arose from the anti-oxidant enzymes. We observed that the basal SOD activity was lower for the HL60/PMA cells than for the two other cell lines and only weak changes were measured after the oxidative treatment. Differences in basal GPx and CAT activities were observed between the three cell lines. A higher GPx activity was measured in the HL60/PMA cells in comparison to the two other proliferative cell lines. This higher GPx activity may be either a consequence of the non-proliferative state of HL60/PMA cells, or due to an intrinsic effect of the PMA, as has been previously reported.[28] Thus, the high GPx activity in HL60/PMA cells could be considered as an adaptive response to the oxidative stress because GPx is able to scavenge hydrogen peroxide.[28,29] Changes in CAT activity due to the oxidative treatment were observed only for HL60 cells. Treatment of these cells by *t*-BHP, which is often considered as a kinetically fast oxidant acting independently of protein synthesis, resulted after 30 min, in an increase of CAT activity, suggesting post-translational mechanisms to regulate this CAT activity. Moreover, this enzyme seems to be implicated in the resistance of leukemia cells to anti-cancer therapy drugs based on redox mechanism, since CAT activity consistently increased in a dose-dependent manner after an *in vitro* hydrogen peroxide treatment of cells.[30]

One of the possible cellular consequences of oxidative stress, examined in this work, is the induction of cell death either by necrosis or apoptosis.[5] The oxidizing agent used in this study, the *t*-BHP, is not only known as a membrane active agent characterized by its rapid and direct action on the cell membrane,[31] but it has also been used as apoptosis inducer in various cellular models.[32] The results of our study confirmed the role of the oxidative stress in apoptosis induction by showing important differences according to the cell proliferation state. The caspase 3 was more strongly expressed in the HL60/PMA cells than in the two other cell lines. This could be related to an increasing expression of several proteases previously reported[12] for HL60 cells after their differentiation into monocytic phenotype. This increase in protease expression may include the caspase 3, as observed in this work. Moreover, the increasing protease expression may also result in the degradation of numerous proteins and could explain the weak PARP expression in HL60/PMA cells and its quasi disappearance after *t*-BHP treatment. Thus, the non-proliferative HL60/PMA cells, treated by *t*-BHP,

did not undergo the apoptotic pathway, but mostly underwent the necrosis pathway. On the contrary, *t*-BHP treatment performed on proliferative THP-1 and HL60 cells resulted mostly in apoptosis, as shown by yopro-1/PI labeling, PARP and caspase 3 cleavages. It is interesting to note that the most proliferative cell line, the HL60 cells also gave the highest percentage of apoptosis, in agreement with the previous works of Moon et al.[13]

The role of thiol compounds in apoptosis induction seems complex. Nevertheless, the low basal GSH and cysteine levels, measured by HPLC in HL60/PMA cells in comparison to HL60 cells, could explain the orientation towards necrosis rather than apoptosis that we observed for cell death in HL60/PMA cells. Such a possibility has already been provided for another cellular model by Re et al.[33]

Our results may be of particular interest in the chemotherapeutic treatments involving an oxidative mechanism since several anti-neoplasic drugs induce apoptosis in leukemia cell lines by oxidant mechanisms.[30,34] Thus, the determination of the response of cells towards oxidative stress, according to their proliferative status, may improve the quality of the evaluation of anti-neoplasic treatments based on a redox mechanism and leading to an apoptotic pathway.[35]

Acknowledgements

The authors thank Professor M.A. Pocidalo and Dr R. Guillot for their fruitful discussions and Ms Vincent from the Centre Technique de Langues (Université Paris 5) for her proofreading of the manuscript. This work was supported by the University Paris 5-René Descartes, the University Paris 7-Denis Diderot and the Fondation pour la Recherche Médicale.

References

[1] Dröge W. Free radicals in the physiological control of cell function. Physiol Rev. 2002;82:47–95.
[2] Halliwell B, Gutteridge JMC. Free radicals in biology and medicine. 3rd edition. New-York: Oxford Science Publication; 2000.
[3] Evans P, Halliwell B. Micronutrients: Oxidant/anti-oxidant status. British J Nutr 2001;85:S67–S74.
[4] Matès JM, Pérez-Gomez C, Nunez de Castro I. Anti-oxidant enzymes and human diseases. Clin Biochem 1999;32:595–603.
[5] Fiers W, Beyaert R, Declercq W, Vandenabeele P. More than one way to die: Apoptosis, necrosis and reactive oxygen damage. Oncogene 1999;18:7719–7730.
[6] Davis W, Jr., Ronai Z, Tew KD. Cellular thiols and reactive oxygen species in drug-induced apoptosis. J Pharmacol Exp Ther 2001;296:1–6.
[7] Plantin-Carrenard E, Braut-Boucher F, Bernard M, Derappe C, Foglietti MJ, Aubery M. Fluorogenic probes applied to the study of induced oxidative stress in the human leukemic HL60 cell line. J Fluorescence 2000;10:167–176.
[8] Fernandes RS, Cotter TG. Apoptosis or necrosis: Intracellular levels of glutathione influence mode of cell death. Biochem Pharmacol 1994;48:675–681.
[9] Sohal RS, Allen RG, Nations C. Oxygen free radicals play a role in cellular differentiation: An hypothesis. J Free Radic Biol Med 1986;2:175–181.
[10] Tsuchiya S, Yamabe M, Yamaguchi Y, Kobayashi Y, Konno T, Tada K. Establishment and characterization of a human acute monocytic leukemia cell line (THP-1). Int J Cancer 1980;26:171–175.
[11] Collins SJ, Gallo RC, Gallagher RE. Continuous growth and differentiation of human myeloid leukaemic cells in suspension culture. Nature 1977;270:347–349.
[12] Rovera G, Santoli D, Damsky C. Human promyelocytic leukemia cells in culture differentiate into macrophage-like cells when treated with a phorbol diester. Proc Natl Acad Sci USA 1979;76:2779–2783.
[13] Moon MS, Lee GC, Kim JH, Yi HA, Bae YS, Lee CH. Human cytomegalovirus induces apoptosis in promonocyte THP-cells but not in promyeloid HL60 cells. Virus Res 2003;94:67–77.
[14] Braut-Boucher F, Aubery M. Fluorescent molecular probes and applications to microspectro-fluorimetry. In: McNeil C, editor. Fluorescence spectroscopy in biochemistry, electronic spectroscopy methods and instrumentation. London: Academic Press; 1999. p 573–582.
[15] Plantin-Carrenard E, Bringuier A, Derappe C, Pichon J, Guillot R, Bernard M, Foglietti MJ, Feldmann G, Aubery M, Braut-Boucher F. A fluorescence microplate assay using yopro-1 to measure apoptosis: Application to HL60 cells submitted to an oxidative stress. Cell Biol Toxicol 2003;19:121–133.
[16] Ahmed N, Williams JF, Weidermann MJ. The human promyelocytic HL60 cell line: A model of myeloid cell differentiation using dimethylsulphoxide, phorbol ester and butyrate. Biochem Int 1991;23:591–602.
[17] McCord JM, Fridovitch I. Superoxide dismutase, an enzymic function for erythrocuprein (hemocuprein). J Biol Chem 1969;244:6049–6055.
[18] Johansson LH, Borg LAH. A spectrometric method for determination of catalase activity in small tissue samples. Anal Biochem 1998;174:331–336.
[19] Lamboley C, Bringuier A, Feldmann G. Induction of apoptosis in normal cultured rat hepatocytes and in Hep3B, a human hepatoma cell line. Cell Biol Toxicol 2000;16:185–200.
[20] Rappeneau S, Baeza-Squiban A, Braut-Boucher F, Aubery M, Gendron MC, Marano F. Use of fluorescent probes to assess the early sulfydryl depletion and oxidative stress induced by mechlorethamine in human bronchial epithelial cells. Toxicol in vitr 1999;13:765–771.
[21] Jacob N, Guillaume L, Garçon L, Foglietti MJ. Dosage de l'homocystéine plasmatique totale et autres aminothiols par chromatographie liquide couplée à la détection par fluorescence. Ann Biol Clin 1987;5:583–591.
[22] Lizard G, Gueldry S, Sordet O, Monier S, Athias A, Miguet C, Bessede G, Lemaire S, Solary E, Gambert P. Glutathione is implied in the control of 7-ketocholesterol-induced apoptosis, which is associated with radical oxygen species production. FASEB J 1998;12:1651–1663.
[23] Andrews NC, Faller DV. A rapid micropreparation technique for extraction of DNA-binding proteins from limiting numbers of mammalian cells. Nucleic Acids Res 1991;19:2499–2500.
[24] Macho A, Hirsch T, Marzo I, Marchetti P, Dallaporta B, Susin SA, Zamzami N, Kroemer G. Glutathione depletion is an early and calcium elevation a late event of thymocyte apoptosis. J Immunol 1997;158:4612–4619.
[25] Pasqualetto V, Néel D, Feugeas JP, Aubery M, Derappe C. HL60 leukaemia cells chemically induced to differentiate retain some surface glycan features of undifferentiated cells not found in normal leukocytes. Glycobiology 1995;5:59–66.

[26] Cotgreave IA, Gerdes RG. Recent trends in glutathione biochemistry—Glutathione-protein interactions: A molecular link between oxidative stress and cell proliferation. Biochem Biophys Res Commun 1998;242:1–9.

[27] Quesada AR, Byrnes RW, Krezoski SO, Petering DH. Direct reaction of H_2O_2 with sulfhydryl groups in HL60 cells: Zinc-metallothionein and other sites. Arch Biochem Biophys 1996;334:241–250.

[28] Bremner TA, D'Costa N, Dickson LA, Asseffa A. A decrease in glucose 6-phosphate deshydrogenase activity and mRNA is an early event in phorbol ester-induced differentiation of THP-1 promonocytic leukemia cells. Life Sci 1996;58:1015–1032.

[29] Cregan SP, Brown DL, Mitchel REJ. Apoptosis and the adaptive response in human lymphocytes. Int J Radiat Biol 1999;75:1087–1094.

[30] Lenehan PF, Gutierrez PL, Wagner JL, Milak N, Fisher GR, Ross DD. Resistance to oxidants associated with elevated catalase activity in HL60 leukemia cells that overexpress multidrug-resistance protein does not contribute to the resistance to daunorubicin manifested by these cells. Cancer Chemother Pharmacol 1995;35:377–386.

[31] Masaki N, Kyle ME, Farber JL. Tert butyl hydroperoxide kills cultured hepatocytes by peroxide membrane lipids. Arch Biochim Biophys 1989;2:390–399.

[32] Haidara K, Morel I, Abalea V, Gascon-Barre M, Denizeau F. Mechanism of tert-butylhydroperoxide induced apoptosis in rat hepatocytes: Involvement of mitochondria and endoplasmic reticulum. Biochim Biophys Acta 2002;1542:173–175.

[33] Re RB, Boucraut J, Samuel D, Birman S, Kerkerian-Le Goff L, Had-Aissouni L. Glutamate transport alteration triggers differentiation-state selective oxidative death of cultured astrocytes: A mechanism different from excitotoxicity depending on intracellular GSH contents. J Neurochem 2003;85:1159–1170.

[34] Kagan VE, Yalowich JC, Borisenko GG, Tyurina YY, Tyurin VA, Thampatty P, Fabisiak JP. Mechanism-based chemopreventive strategies against etoposide-induced acute myeloid leukemia: Free radical/anti-oxidant approach. Mol Pharmacol 1999;56:494–506.

[35] Matès JM, Sanchez-Jimenez FM. Role of reactive oxygen species in apoptosis: Implications for cancer therapy. Int J Biochem Cell Biol 2000;32:157–170.